

Research Article: Negative Results | Cognition and Behavior

# Long-range alpha-synchronisation as control signal for BCI: A feasibility study

#### https://doi.org/10.1523/ENEURO.0203-22.2023

Cite as: eNeuro 2023; 10.1523/ENEURO.0203-22.2023

Received: 25 May 2022 Revised: 15 December 2022 Accepted: 10 January 2023

This Early Release article has been peer-reviewed and accepted, but has not been through the composition and copyediting processes. The final version may differ slightly in style or formatting and will contain links to any extended data.

Alerts: Sign up at www.eneuro.org/alerts to receive customized email alerts when the fully formatted version of this article is published.

Copyright © 2023 Esparza-laizzo et al.

This is an open-access article distributed under the terms of the Creative Commons Attribution 4.0 International license, which permits unrestricted use, distribution and reproduction in any medium provided that the original work is properly attributed.

#### 1 **1. Manuscript Title (50 word maximum)**

2 Long-range alpha-synchronisation as control signal for BCI: A feasibility study.

#### 3 2. Abbreviated Title (50 character maximum)

4 Alpha-synchronisation in BCI control

## 3. List all Author Names and Affiliations in order as they would appear in the published article

Authors: Martín Esparza-Iaizzo<sup>1</sup>, Irene Vigué-Guix<sup>1</sup>, Manuela Ruzzoli<sup>2,3</sup>,
 Mireia Torralba<sup>1</sup>, Salvador Soto-Faraco<sup>1,4</sup>.

Affiliations: <sup>1</sup>Center for Brain and Cognition, Universitat Pompeu Fabra,
 Barcelona, Spain; <sup>2</sup>Basque Center on Cognition Brain and Language (BCBL),
 Donostia/San Sebastián, Spain. <sup>3</sup>Ikerbasque, Basque Foundation for Science,
 Bilbao, Spain. <sup>4</sup>Institució Catalana de Recerca i Estudis Avançats (ICREA),
 Barcelona, Spain.

#### 14 4. Author Contributions

MEI and IVG Performed research, Analysed the data; MR Analysed data; MT
 and SSF Designed research; MEI, IVG, MT, MR and SSF Wrote the paper.

#### 17 5. Correspondence should be addressed to (include email address)

- Salvador Soto-Faraco, Universitat Pompeu Fabra, Room 24.327, Ed. Mercè
   Rodoreda, Carrer de Ramón Trias Fargas, 25-27, 08005 Barcelona, Spain.
- 20 Email: salvador.soto@upf.edu
- 21 6. Number of Figures: 5
- 22 **7. Number of Tables:** 0
  - 8. Number of Multimedia: 0
- 24 9. Number of Extended Data Figures: 6
- 25 **10. Number of words for Abstract:** 210
- 26 **11. Number of words for Significance Statement:** 112
- 27 **12. Number of words for Introduction:** 749
- 28 **13. Number of words for Discussion:** 2612
- 29 14. Acknowledgements: Authors report no acknowledgments
- 30 15. Conflict of Interest: Authors report no conflict of interest
- 31 **16. Funding sources:** This research was supported by AGAUR *Generalitat de*
- 32 Catalunya (2017 SGR 1545). This project has been co-funded with 50% by
- 33 the European Regional Development Fund under the framework of the

5

6

FEDER Operative Programme for Catalunya 2014-2020 Ministerio de Ciencia
 e Innovación (Ref: PID2019-108531GB-I00 AEI/FEDER).

## 1 KEYWORDS

Brain-Computer Interface; Alpha; EEG; Oscillations; Visuospatial Attention; Phase
Coupling.

## 4 ABSTRACT

5 Shifts in spatial attention are associated with variations in alpha-band ( $\alpha$ , 8–14 Hz) 6 activity, specifically in inter-hemispheric imbalance. The underlying mechanism is 7 attributed to local  $\alpha$ -synchronisation, which regulates local inhibition of neural 8 excitability, and fronto-parietal synchronisation reflecting long-range communication. 9 The direction-specific nature of this neural correlate brings forward its potential as a 10 control signal in brain-computer interfaces (BCI). In the present study, we explored 11 whether long-range  $\alpha$ -synchronisation presents lateralised patterns dependent on 12 voluntary attention orienting and whether these neural patterns can be picked up at a 13 single-trial level to provide a control signal for active BCI. We collected 14 electroencephalography (EEG) data from a cohort of healthy adults (n = 10) while 15 performing a covert visuospatial attention (CVSA) task. The data shows a lateralised 16 pattern of  $\alpha$ -band phase coupling between frontal and parieto-occipital regions after 17 target presentation, replicating previous findings. This pattern, however, was not 18 evident during the cue-to-target orienting interval, the ideal time window for BCI. 19 Furthermore, decoding the direction of attention trial-by-trial from cue-locked 20 synchronisation with support vector machines (SVM) was at chance-level. The present 21 findings suggest EEG may not be capable of detecting long-range  $\alpha$ -synchronisation 22 in attentional orienting on a single-trial basis and, thus, highlight the limitations of this 23 metric as a reliable signal for BCI control.

## 24 SIGNIFICANCE STATEMENT

Cognitive neuroscience advances should ideally have a real-world impact, with an 25 obvious avenue for transference being BCI applications. The hope is to faithfully 26 27 translate user-generated brain endogenous states into control signals to actuate 28 devices. A paramount challenge for transfer is to move from group-level, multi-trial 29 average approaches to single-trial level. Here, we evaluated the feasibility of single-30 trial estimation of phase synchrony across distant brain regions. Although many 31 studies link attention to long-range synchrony modulation, this metric has never been 32 used to control BCI. We present a first attempt of a synchrony-based BCI that, albeit 33 unsuccessful, should help break new ground to map endogenous attention shifts to 34 real-time control of brain-computer actuated systems.

## 35 INTRODUCTION

A few decades ago, imagining an interface between the human brain and a computer 36 37 was closer to science fiction than to scientific achievement. Nowadays, brain-computer 38 interfaces (BCIs) can read out brain activity, extract features from the signal in real-39 time, and convert them into outputs for monitoring, controlling devices, or even 40 modifying cognitive states (Blankertz et al. 2016). One significant challenge of BCIs is finding reliable control signals from brain activity with a sufficiently high signal-to-noise 41 42 ratio (SNR) at a trial-by-trial level to allow successful classification. Ideally, the 43 appearance of the target brain activity should depend on endogenous mental states 44 that a user can control at will. The use of non-invasive, cost-effective, and light-weight 45 neuroimaging devices can, in turn, facilitate transfer to real applications. For now, EEG 46 is the most viable candidate to achieve real-life BCI.

eNeuro Accepted Manuscript

47 For example, some EEG-based BCIs have used motor imagery as a control signal 48 (e.g., imagined right/left-limb movement; Padfield et al. 2019), whereas others have 49 used neural correlates of covert visuospatial attention (CVSA) (van Gerven and 50 Jensen 2009; Treder et al. 2011; Tonin et al. 2013). Here, we will concentrate on the 51 latter. In human behaviour, CVSA is used to direct processing resources to relevant 52 locations in the environment whilst disengaging from irrelevant locations (Pashler 53 1999; Foster and Awh 2019). CVSA can be manipulated through a Posner cueing 54 protocol (Posner 1980), which shows a robust effect on behavioural performance: 55 higher accuracy and faster reaction times for targets appearing at the cued (attended) 56 location compared to targets appearing in un-cued, putatively unattended locations 57 (Posner 1980).

58 Shifts in CVSA are associated with changes in oscillatory activity in the alpha-band ( $\alpha$ , 59 8–14 Hz) at parieto-occipital regions (Klimesch 1999; Foster et al. 2017). Typically,  $\alpha$ -60 power shows an inter-hemispheric imbalance when attention is covertly oriented to 61 either the left or right visual field, revealing its potential as a control signal for BCI 62 implementations (Rihs et al. 2007; Thut et al. 2006, see Astrand et al. 2014b for a 63 review). Inter-hemispheric  $\alpha$ -power imbalance corresponds to a late process in CSVA 64 shifts (van Diepen et al. 2019). First, cueing information is integrated through sensory 65 pathways in a bottom-up fashion, reaching higher visual areas in the parietal cortex 66 (e.g., intraparietal sulcus) and eventually frontal regions (e.g., frontal eye fields) 67 (Petersen and Posner 2012). From there on, top-down modulation shifts attention to 68 the corresponding hemifield, where it is maintained during target anticipation (Simpson 69 et al., 2012). The mechanism involved in this top-down modulation is thought to involve 70 long-range  $\alpha$ -synchronisation between the frontal and posterior cortex, which 71 eventually leads to classical inter-hemispheric imbalances in  $\alpha$ -power observed in the

72 visual cortex (Sauseng et al. 2005; Doesburg et al. 2009, Lobier et al. 2018). Long-73 range synchronisation is a potential mechanism to increase the fidelity and 74 effectiveness of communication throughout the brain (Clayton et al. 2018) among 75 occipital, parietal, and frontal regions (Sadaghiani and Kleinschmidt 2016). 76 Synchronising excitability cycles between distant neural populations increases the 77 likelihood of spikes from one region discharging post-synaptic potentials during a 78 specific (excitable) phase of the other (Fries, 2015). Despite the evidence supporting 79 this model (Buschman and Miller., 2007; Cardin et al., 2009), there is still debate on 80 its temporal dynamics, lateralisation patterns and individual-level variability.

81 Despite the evidence of links between long-range  $\alpha$ -synchronisation and behavioural 82 performance at group-level analyses (Sauseng et al. 2005; Doesburg et al. 2009; 83 Doesburg et al. 2016), BCI protocols based on endogenous attention orienting have 84 only used  $\alpha$ -power as a control signal. In our study, we attempt to replicate a previously 85 demonstrated effect in attention orienting involving long-range  $\alpha$ -synchronisation to 86 assess its feasibility in BCI paradigms. The original publication (Sauseng et al., 2005) 87 found significant increases in contralateral over ipsilateral connectivity around the time 88 of target appearance. We hypothesized that, if attention-driven connectivity emerged 89 in target-centered time windows, it may also be present in the cue-to-target interval, 90 where participants are putatively shifting attention towards the cued side. Further, this 91 cue-to-target time window would enable the use of long-range  $\alpha$ -synchronisation in 92 BCIs based on purely endogenous brain signals. Therefore, we will test whether such 93 contra- and ipsilateral patterns in  $\alpha$ -synchronisation emerge in single-trial dynamics 94 with sufficient signal strength to make them a reliable control signal. To do so, we used 95 an EEG dataset from a lateralised endogenous spatial attention task to replicate 96 group-level effects found by Sauseng et al. (2005), to explore the cue-to-target

97 interval, and to classify the direction of attention at the single-trial level using long98 range α-phase synchronisation as proof of concept for transference to BCI.

## 99 MATERIALS AND METHODS

#### 100 Participants

We used data from a previous, unrelated study (Torralba et al 2016). The dataset consisted of 15 participants (mean age = 22, SD = 3; 7 female). All participants provided informed consent and had a normal or corrected-to-normal vision. The study was ran in accordance with the Declaration of Helsinki and the experimental protocol approved by the local ethics committee CEIC Parc de Salut Mar (Barcelona, Spain).

#### 106 **Task**

107 Before the experimental session, the participant's EEG activity was recorded during a 108 five-minute recording at rest with eyes closed to extract the individual  $\alpha$  frequency 109 (IAF) used in the analyses. In the experimental session, participants performed a 110 modified version of the Posner cueing task (see Figure 1A). The trial started with the 111 onset of a central fixation cross, placed between two placeholders located 20° of visual 112 angle left and right off-centre, vertically shifted 20° of visual angle below the fixation 113 cross (see Figure 1A). After 200 ms fixation period, a central auditory cue (100 ms 114 duration) indicated the likely target location through either high pitch (2000 Hz) or low 115 pitch (500 Hz) tones, the mapping was randomised across subjects. Participants 116 should covertly attend to the indicated side, without moving their eyes, during a jittered 117 inter-stimulus interval (ISI; 2000 ± 500 ms). The use of a jittered ISI was employed in 118 order to avoid participants using automatic temporal attention to solve the task. Next, 119 the target (a Gabor grating tilted 45° left or right, 50 ms duration) appeared briefly 120 inside one of the placeholders, with 75% validity regarding the cued location. The 121 grating contrast was adjusted individually, as described below. A noise pattern with an 122 equal overall luminance as the target was presented at the alternative placeholder, 123 with the exact timings as the target. Participants were asked first to indicate if they had 124 detected the target (yes/no detection) and, subsequently, the target's tilt (left/right 125 discrimination). Both answers were made by keypress, in an un-speeded fashion, and 126 with response mapping (top-bottom) orthogonal to the attention manipulation and 127 varied from trial to trial. A trial was considered correctly answered only when 128 participants both detected the stimulus and discriminated the hemifield in which it was 129 presented. An inter-trial interval of 1000 ms followed the response, and a new trial 130 began. Unless otherwise noted, the EEG analyses were done on validly cued trials 131 that responded correctly. On average,  $289.9 \pm 11.3$  trials from each participant were 132 employed for the EEG analysis.

133 The Gabor gratings used as stimuli were 0.002 cycles per degree, with a size of 3.35°, 134 embedded in white noise. The contrast was adjusted individually using a preliminary 135 threshold titration procedure in which thresholds for both sides (left and right) were 136 independently adjusted to a 70% detection rate when cued (in the attended location). 137 Stimuli were presented on a 21" CRT screen with a refresh rate of 100 Hz and a 138 resolution of 1024 x 768 pixels. The experiment was implemented in MATLAB R2015b 139 (MATLAB, RRID: SCR\_001622) using the Psychophysics Toolbox (Psychophysics 140 Toolbox, RRID: SCR\_002881).

#### 141 EEG recording and pre-processing

EEG recordings were obtained from 64 Ag/AgCl electrodes positioned according to the 10-10 system with AFz as ground and nose tip as reference. Impedance was kept below 10 kΩ. The employed system was an active actiCHAmp EEG amplifier from Brain Products (Munich, Germany). The signal was sampled at 500 Hz and processed in MATLAB 2020 and 2015 (MATLAB, RRID: SCR\_001622) using custom functions and the FieldTrip toolbox (FieldTrip, RRID: SCR\_004849).

Manual artefact rejection was applied to discard trials where any EOG components 148 had an amplitude higher than 50  $\mu$ V. Defective channels were repaired using 149 150 neighbours calculated by triangulation and splines for interpolating channel data. 151 Then, the data was demeaned and notch filtered at 50 Hz to exclude line noise. Next, 152 fifth-order high-pass and sixteenth-order low-pass IIR Butterworth filters were 153 employed to limit the signal between 0.16 and 45 Hz (Sauseng et al. 2005). The 154 filtering was done forward and backwards (two-pass), which resulted in zero phase 155 lag.

#### 156 Time-frequency analysis

157 We performed long-range synchronisation analyses in two time windows. The first was 158 time-locked to the target onset (target-locked) to replicate Sauseng et al. (2005) 159 methods and validate our analysis pipeline. The second was time-locked to the cue 160 onset (cue-locked) to estimate long-range  $\alpha$ -phase synchronisation during covert 161 visuospatial attention shifts.

162 Following Sauseng et al. (2005), for the target-locked analysis, we used two windows 163 of 200 ms: a pre-target (-200 to 0 ms) and a post-target window (200 ms to 400 ms). 164 The latter excludes the interval 0 to 200 ms, most affected by the phase resetting effect 165 of target presentation. For the cue-locked analysis, we used the cue-to-target time 166 window between 500 ms and 1500 ms post-cue and divided it into five consecutive 167 and non-overlapping 200 ms windows. By analysing from 500 ms onwards we avoid 168 the event related potential (ERP) caused by cue presentation and allow endogenous 169 attention shift to build up, a process which takes a few hundreds of milliseconds (Foxe 170 and Snyder 2011). The cue-locked analysis period ends at 1500 ms, which was the 171 minimum possible duration of the cue-to-target interval (duration of  $2000 \pm 500$  ms, 172 see methods). All epoched data was mirror-reflected to avoid edge artefacts (Cohen 173 2014) when performing the time-frequency analysis. Afterwards, data were trimmed, 174 and reflected edges were removed.

We computed the Fourier coefficients using 5-cycle Morlet wavelets (Grossmann and Morlet 1984) with 16 logarithmically spaced frequencies ranging from 2.6 Hz to 42 Hz. For the analysis aimed at replicating Sauseng's results, we only used wavelets within the upper α-band (9.54 - 14.31 Hz) (Sauseng et al. 2005), whereas, for the exploratory analysis, we used the whole frequency range (i.e., 2.6 - 42 Hz) to explore further longrange α-phase synchronisation in other frequency bands beyond the IAF.

#### 181 Connectivity measures

Three clusters of electrodes of interest (EOI) were defined for the connectivity
analyses, mimicking Sauseng et al., 2005: A fronto-medial (FM) EOI cluster (Fz, FC1,
FC2) and two symmetric posterior clusters located either atthe parietal left (PL) region

(P3, PO3, PO1) or the parietal right (PR) region (P4, PO4, PO2). To infer connectivity
between each parietal EOI cluster and the FM location, we used Phase Locking Value
(PLV) (Lachaux et al. 1999). This metric reports the consistency of phase differences
between two locations across multiple trials and is not affected by power differences.
Mathematically, the PLV is expressed as the absolute value of the average complex
unit-length phase differences:

191 
$$PLV(x,y) = \left| \frac{1}{n} \sum_{k=1}^{n} e^{i(\varphi_{x}(k) - \varphi_{y}(k))} \right|$$
(1)

192 where *n* corresponds to the total number of trials indexed by *k* and  $\varphi_x$ ,  $\varphi_y$  correspond 193 to the phases at electrodes x and y, respectively. PLV was calculated according to 194 equation (1) using the phases for every combination of individual electrode pairs of the 195 FM-PR and FM-PL networks. Then, these values were averaged, resulting in a time 196 series of PLV FM-PR and FM-PL networks for each of the frequencies of interest and 197 condition (attended left and attended right) trials. Subsequently, the PLV time series 198 were collapsed as either ipsilateral (FM-PL network and attend left; FM-PR and attend 199 right) or contralateral (FM-PR network and attend left; FM-PL and attend right). 200 Therefore, for each participant and frequency of interest, two time series of PLV were 201 obtained (contra- and ipsilateral PLV).

### 202 Classification

The trial classification was performed using support vector machines (SVM). We selected FM-PR and FM-PL connectivity as input to the SVM. *Attended right* and *attended left* labels for each trial were provided as ground truth for the algorithm. The main goal of the classifier was to infer, on each trial, whether a participant was 207 attending on the left or right hemifield, based on the long-range  $\alpha$ -phase 208 synchronisation in the left and right fronto-parietal networks. Note that PLV is 209 computed across trials, and SVM aims to classify on a single-trial basis, so PLV was 210 also calculated across time points (Cohen 2015). As a validation step, we repeated 211 the target-locked analysis employing this metric (i.e., cross-time PLV) before 212 proceeding with the cue-locked classification attempt.

213 We divided the cue-locked interval ranging from 500 to 1500 ms in bins of 200 ms, 214 yielding five values for FM-PR connectivity and five for FM-PL connectivity. The 215 resulting ten values were used as input to the SVM to perform the optimisation and 216 classification of the trials. Note that for the classification, we used the data from the 217 participant that achieved a significant difference in PLV values between parietal left 218 and right EOI clusters in all cue-to-target windows (P10). Trials were split into a training 219 (80%) and testing (20%) set of trials to avoid overfitting. Then, the training set was 220 subdivided into sub-training (80%) and validation sets (20%).

221 Our initial approach was to use a linear kernel for the classification. However, after 222 evaluating the option through cross-validation of the validation set and obtaining a 223 negative result (i.e., classification was not better than chance level), we decided to use 224 a Gaussian kernel (i.e., Radial Basis Function). In order to select the most suitable 225 and efficient values for classifying attended left and attended right trials from the 226 validation set, we optimised the parametric space of the SVM. This comprised margin and gamma (y) parameters, which were explored in logarithmic steps from 10<sup>-6</sup> to 10<sup>3</sup> 227 228 for both constants and every fold.

#### 229 Inter-hemispheric power imbalance analysis

230 Besides calculating the long-range  $\alpha$ -phase coupling, we also computed the inter-231 hemispheric  $\alpha$ -power imbalance at parietal regions, both at the individual and at group-232 level, as a reality check. For this reality check, we used Thut et al., (2006) for guidance 233 to choose the electrodes of interest. First, we performed an independent component 234 analysis (ICA), during which 3±1 components were discarded on average per 235 participant, based on a visual inspection, the components' topography, and time 236 course. The rejected components comprised both ocular and motor artifacts. Please 237 note that ICA was only performed for the power analysis, not for the connectivity 238 pipeline, in order to replicate the exact pre-processing as seen in Sauseng et al., 239 (2005) and, importantly, because phase of electrophysiological recordings is affected 240 when ICA are rejected (Thatcher et al., 2020).

241 The frequency of interest used in lateralisation analyses was adjusted for each 242 participant depending on the individual  $\alpha$  frequency (IAF) extracted from the five-243 minute recording (eyes closed) previous to the experiment (see above). The IAF was 244 determined based on the presence of a single peak (i.e., a local maximum) within the 245 considered frequency band of interest (5-15 Hz) on the power spectrum density (PSD). 246 A spectrogram was extracted for each parieto-occipital electrode (P7, P5, P3, P1, Pz, 247 P2, P4, P6, P8, PO3, PO4, POz, PO9, PO10, O1, Oz, O2) using the Welch method 248 (segments of 1000 ms with a 10% overlap, a Hanning taper to avoid spectral leakage 249 and 0.25 Hz frequency resolution). The power spectrum was averaged across 250 electrodes for each participant and normalised by the mean power from 1 to 40 Hz 251 (Vigué-Guix et al., 2022).

252 To extract the  $\alpha$ -power during the task, we selected the epoch from -1.5 to 3 s in cue-253 locked trials by convolving the EEG signal with a set of complex Morlet wavelets 254 (Grossmann and Morlet 1984) of 5 cycles (nc). The frequencies of the wavelets ranged 255 from IAF ± 1 Hz, in 1 Hz steps. For instance, an IAF peak of 10 Hz would have a 256 bandwidth ranging from 8.33 Hz to 11.67 Hz. Power was extracted from two symmetric 257 regions of interest precisely in PR (P6, P8, PO4, O2) and PL locations (P5, P7, PO3, 258 O1) in order to replicate as closely as possible the original EOI electrodes used in Thut 259 et al., (2006). Power imbalance was computed according to the formula:

260 
$$Lateralization \ Index = \frac{\alpha(PR \ EOI) - \alpha(PL \ EOI)}{mean \ of \ \alpha(PL + PR \ EOI)}$$
(2)

where  $\alpha$  (PL EOI) and  $\alpha$  (PR EOI) are the average of  $\alpha$ -power over left and right electrodes of interest, respectively. Equation (2) leads to smaller (negative) values where  $\alpha$ -activity is more prominent over the left hemisphere than the right ( $\alpha$  (PL EOI) >  $\alpha$  (PR EOI)) and to larger (positive) values for the opposite pattern ( $\alpha$  (PL EOI) <  $\alpha$ (PR EOI)). According to theory and previous findings, values of LI reflecting attention directed to the right hemifield should be larger than LI values reflecting leftward directed attention.

Finally, we also checked whether there was any relationship between the  $\alpha$ -power imbalance and the contra-ipsi difference of PLV for each attended location. We explored the correlations between  $\alpha$ -lateralisation indexes and the effect in PLV contra-ipsi differences at the pre-target (-200 to 0 ms) and post-target (200 to 400 ms) windows using Pearson correlations.

#### 273 Statistical analyses

274 A one-tailed nonparametric Monte Carlo permutation test was computed to determine 275 significant differences in PLV between networks for each attended location (Mostame 276 et al. 2019). For each participant, the attended right or left labels were randomly 277 assigned to trials, and surrogate PLVs were calculated from the resulting dataset. This 278 process was repeated 10,000 times (iterations) to create a null distribution of PLV 279 values. The obtained p-value corresponded to the proportion of surrogate iterations 280 with a contra-ipsi difference larger than the actual measured value (one-tailed test). 281 This process was performed on every time window defined in the previous section. 282 For the group analysis, the procedure was equivalent, but surrogate PLV distributions 283 were averaged across participants before the statistical test.

For the statistical assessment of the *a*-power imbalance over time between attended 284 285 *left* and *attended right* trials, we performed a cluster-based permutation test procedure 286 (100,000 randomisations) for each participant and at the group-level (one-tailed 287 permutation test) (Maris and Oostenveld 2007; Meyer et al. 2021). We assessed that 288 lateralisation indexes for attended right and attended left trials were two significantly 289 different distributions by applying a one-tailed t-test (independent samples) with  $\alpha$ -290 level = 0.05 for each participant. At group-level, we performed a one-tailed paired t-291 test with the mean lateralisation indexes for attended right and attended left trials for 292 each participant with  $\alpha$ -level = 0.05. Correlations between  $\alpha$ -power imbalance and the 293 contra-ipsi difference of PLV were corrected for multiple comparisons by applying the 294 False Discovery Rate (FDR) of Benjamini and Hochberg (Benjamini and Hochberg 295 1995).

## 296 **RESULTS**

#### 297 Behavioural results

298 Five participants who presented equivalent detection and discrimination rates for 299 stimuli appearing at cued and un-cued locations were discarded from the analysis. 300 leaving a total of 10 participants. As expected, behavioural results showed that the 301 detection rate calculated based on both the detection response (Yes/No) and the 302 discrimination response (Left/Right; chance level at 0.25) was superior for cued 303 (attended) trials  $0.68 \pm SEM = 0.02$  compared to un-cued (unattended) ones  $0.46 \pm 0.04$ 304 (see, Figure 1B). The pattern on each hemifield was equivalent: on the left hemifield 305 attended =  $0.68 \pm 0.03$  and unattended =  $0.47 \pm 0.03$ ; for the right hemifield attended 306  $= 0.67 \pm 0.03$ , and unattended  $= 0.44 \pm 0.06$ . We used one tailed t-tests to assess that 307 performance was above chance level (25%) for each of the conditions (attended and 308 unattended) and hemifields separately: Attended Left trials (0.68±0.11, p-value=2.10<sup>-</sup> 309 <sup>7</sup>, t(9)=12.593), Attended Right trials (0.67 $\pm$ 0.11, p-value=3 $\cdot$ 10<sup>-7</sup>, t(9)=12.226), Unattended Left trials (0.47±0.08, p-value=5.10<sup>-6</sup>, t(9)=8.876) and Unattended Right 310 311 trials (0.44±0.20, p-value=0.06, t(9)=3.117).

#### Target-locked long-range $\alpha$ synchrony

313 Here, we describe the results from the target-locked analysis, carried out to reproduce 314 Sauseng et al.'s (2005) findings. Long-range synchrony was estimated using PLV 315 between frontal EOI and each of two lateralised parietal EOI. **Figure 2** shows the 316 group-level connectivity analysis of the upper  $\alpha$ -band (9.54 - 14.31 Hz). Phase 317 coupling is depicted as the mean across the pre-target window (-200 to 0 s) and the 318 post-target window (200 to 400 ms), as well the temporal course (from to -500 to 500 319 ms). Regarding the left fronto-parietal network (Figure 2A left), PLV was consistently 320 higher when attention was directed rightward (contralateral) than leftward (ipsilateral) 321 in both pre-target and post-target windows, although the PLV difference only reached 322 significance in the post-target window (p < 0.05). Regarding the right network (Figure 323 **2A right)**, PLV was stronger when attention was directed leftward (contralateral) than 324 rightward (ipsilateral) in the post-target window, whereas the pre-target window does 325 not show this difference. Neither window, however, emerged as significant. This 326 pattern generally replicates Sauseng et al. (2005) results, as indicated by the dashed 327 lines in **Figure 2A** representing the mean phase-coupling from their study. Lower 328 panels in Figure 2A display the temporal course of phase coupling to provide a time-329 resolved illustration of the phase-coupling effect. For the attended right condition, PLV 330 values in the left network should be higher than PLV values for the attended left. The 331 inverse pattern should hold in the right network. Moreover, Figure 2B presents the 332 PLV with side of attention collapsed as contra- and ipsilateral with respect to the 333 corresponding network. Individual PLV values, marked as black dotted line s, exhibit 334 a consistent contra- to ipsilateral increase in the post-target window. Group-level 335 statistical analysis further showcased a significant difference limited to this time 336 window (200 to 400 ms, p < 0.05). This result was controlled by avoiding the pre-337 processing band-pass filter which may affect phase estimation, and by computing a 338 Hjorth filter to avoid the effects of volume conduction (Hjorth 1975). Both analyses 339 maintained the significant differences between contralateral and ipsilateral PLV (p < p340 0.05).

At individual level, only 3 out of 10 participants showed significant contralateral PLV increase (P02, p < 0.01; P05, p < 0.01; P07, p < 0.01; see **Figure 2-1**). The lack of a

significant group-level effects in the pre-target window is consistent with individual phase coupling, as a multiple subject present a trend in the opposite direction as expected (i.e., ipsilateral over contralateral PLV; see **Figure 2-1**). We further assessed single-subject synchronization through the phase linearity measurement (PLM) as it has been recently reported to be a robust metric for trial-level connectivity (Baselice et al., 2018). We did not find any significant effects in any participant (p > 0.05; see **Figure 2-2**).

#### 350 **Cue-locked long-range** *α* synchrony

351 In the previous section, we replicated the results as in Sauseng et al., (2005). The 352 findings from here onwards correspond to original results to ascertain whether 353 attention-based long-range connectivity during the attention-orienting period could be 354 a reliable signal for BCI control. We explored the cue-to-target interval before target 355 presentation (500 ms to 1500 ms after cue onset). Considering that the cue indicates 356 the hemifield to which participants should voluntarily lateralise attention, differences in 357 contralateral and ipsilateral connectivity may potentially emerge in this time window. 358 So far, we have seen that attention shifts had significant consequences on behaviour 359 and target processing (post-target connectivity). At the group level, however, no 360 significant difference between contralateral and ipsilateral connectivity in the upper  $\alpha$ -361 band was found in any of the five 200 ms time windows considered in the cue-to-target 362 period (see Figure 3A). At the individual level, 7 participants had a significant 363 contralateral PLV increase in at least in one window (see Figure 3-1). However, only 364 one participant (P10) showed this effect in all time windows and, furthermore, did not 365 present a significantly higher contralateral connectivity in pre-target and post-target 366 time windows of the target-locked analysis.

367 We chose the upper  $\alpha$ -band a priori given Sauseng et al. (2005)' findings, as well as 368 the effects in the target-locked analyses from the present dataset. However, we 369 conducted additional analyses to explore other frequencies (between 2.4 and 42 Hz) 370 in search of differences between contralateral and ipsilateral PLV (see, Figure 3B). 371 Values were collapsed as the difference between both measures (contra-ipsi) and z-372 scored. Over time, neither clear trends across frequencies nor apparent increases 373 were observed in contralateral or ipsilateral connectivity. Individual results showed the 374 same trend and did not present relevant PLV patterns in any participant beyond those 375 from upper  $\alpha$ -band findings in P10 (see **Figure 3-2**).

#### 376 Classification

The results are hardly promising in generalising the use of long-range connectivity for BCI control. However, BCI protocols are often very sensitive to individual patterns. Here, we intended to seek a proof-of-concept, from at least a single participant. With this goal in mind, we attempted single-trial classification, as either *attended right* or *attended left*, according to cue-locked connectivity patterns. We selected the participant (P10) for whom we found significant connectivity differences in the cue-totarget time window of the cue-locked analysis. The total number of trials was 338.

We carried out a validation of cross-time PLV in the target-locked window to understand whether this metric could replicate group-level differences between contraand ipsilateral networks found through cross-trial PLV. These results can be seen in **Figure 4A**. Statistical analysis showed no significant differences between contra- and ipsilateral scenarios in either time window. Individual values were also non-significant (see **Figure 4-1**). Considering the large parametric landscape of SVM

implementations, we optimised the gamma and margin parameters of a Gaussian kernel (see **Figure 4B**). From a qualitative perspective, no clear maximum validation accuracy values emerge from the landscape, although quantitative analysis identified minimum values of margin and  $\gamma$  to be used on the test set in every fold. The lack of a clear minimum suggests that the model may be unable to classify individual trials regardless of the parametric values.

396 Ten-fold cross-validation was carried out to maximise the available data and improve 397 the classification accuracy. Single trials predicted as either attended right or attended 398 left were contrasted with the actual cue direction in each trial. Classification outcomes 399 are shown in Figure 4C, which resulted in virtually chance-level sorting (0.541). The 400 confusion matrix displays the distribution of each class, revealing the skewed 401 distribution of values towards attended right labels, which is far from the ideal 402 clustering along the diagonal of the matrix. Finally, we employed two additional 403 algorithms to classify both attended right and attended left trials. These consisted of 404 shrinkage linear discriminant analysis (sLDA) and Riemannian minimum distance to 405 the mean (RMDM), as they are shown to work well in small training sets (Lotte et al., 406 2018). Both decoding techniques yielded chance-level results (see Figure 4-2)

#### 407 Inter-hemispheric power imbalance

As a reality check on the dataset, we addressed whether there was a difference in the 409  $\alpha$ -power inter-hemispheric imbalance between *attended left* and *attended right* trials. 410 We performed the cue-locked analysis at the group level, using the Lateralization 411 Index (LI) described by Thut et al. (2006) (see **Figure 5A).** On average, the 412 lateralisation index was significantly different between *attended right* and *attended left* 

413 in the expected direction (p < 0.01, Cohen's d = -0.8356). At the individual level, 7 out 414 of the 10 participants showed a significant difference in lateralisation index between 415 the two attention conditions (p < 0.05; see **Figure 5-1**). We also performed a time-416 resolved version of this analysis within the cue-to-target window. A cluster-based 417 permutation test (Figure 5B) showed significance within two time periods, from 0.66 418 to 0.82 s and 1.34 to 1.5 s. At the individual level, only for one participant (P01), the 419 cluster-based permutation test revealed a significant cluster over time from 0.6 to 1 s 420 (see Figure 5-1). These results are consistent with the results of previous studies (e.g., 421 Tonin et al. 2012; Thut et al. 2006), at least at the group level. It is more challenging 422 to compare single-subject data with other studies, as it usually is not reported or 423 statistically analysed.

424 Finally, we explored the potential correlation between  $\alpha$ -power inter-hemispheric 425 imbalance measured with the lateralization index and  $\alpha$ -phase coupling for each 426 attended location (see Figure 5 C-D). In the pre-target window (Figure 5C), the 427 correlations for attended right (r = -0.25, p > 0.05) and attended left (r = -0.13, p >428 0.05) did not reach significance. Neither did the correlations for attended right (r = -429 0.44, p > 0.05) and attended left (r = -0.42, p > 0.05) at the post-target (Figure 5D) 430 window. A visual inspection indicated that participants showing an effect in PLV 431 contra-ipsi differences are below the correlation fit in pre-target and post-target 432 windows, suggesting that those participants have a more negative effect in PLV 433 contra-ipsi differences.

## 434 **DISCUSSION**

435 The present study addressed the relationship between shifts in visuospatial attention 436 and the lateralisation of  $\alpha$ -band coherence between frontal and parietal electrodes, to 437 assess their feasibility as a control signal in BCI. Previous studies, using group-438 averaged multi-trial analyses, found increased long-range  $\alpha$ -synchronisation in the 439 hemisphere contralateral to the attended hemifield, and suggested that it reflects top-440 down mechanisms of visual spatial attention (Sauseng et al., 2005; Doesburg et al., 441 2009). We reasoned that if contra- to ipsilateral differences in synchronisation would 442 emerge as a result of endogenous top-down mechanisms, they should be present 443 following cue presentation as participants shift their attention. This hypothesis stems 444 from how instructing participants to shift their attention laterally before target 445 appearance engages frontoparietal visual processing pathways (Corbetta and 446 Shulman 2002; Hopfinger et al. 2000; Asplund et al. 2010). Here, we sought proof that 447 long-range neural synchronisation engaged in this network could be used for BCI 448 control on a trial-by-trial basis.

In attention-orienting protocols, the cue-to-target period offers the possibility of implementing a BCI control in anticipation of the target appearance. This would open the possibility of designing active BCI systems controlled by the user's voluntary decision to attend left/ rightward covertly. Therefore, our study employed long-range  $\alpha$ -synchronisation in the frontoparietal network (FPN) as means to investigate whether this brain measure could potentially discriminate attended locations of the left/right visual field.

We found significant group-level differences in contra- to ipsilateral long-range  $\alpha$ synchronisation around target onset, replicating Sauseng et al. (2005). These results demonstrate the involvement of lateralised long-range  $\alpha$ -synchrony along the FPN during the post-target period and especially reveal the potential of EEG to grasp these effects, at the group level. However, similar differences in fronto-parietal synchrony

461 were not observed during the cue-to-target time window, which was the time of interest 462 for BCI purposes. We also extended the cue-locked analysis to other frequencies 463 outside the  $\alpha$ -band, with equally negative results. Finally, given the high individual 464 variability of single-trial analysis outcomes, we attempted to classify the individual trials 465 of one selected participant for whom significant synchronisation differences following 466 cue presentation were found, as a benchmarking process. The results nevertheless 467 rendered chance-level classification. Below, we discuss how these results may be 468 influenced by various methodological aspects (e.g., different time windows, classifier's 469 input metric) and how they fit into state-of-the-art literature. Please note that because 470 the focus of our study was on single-trial analysis, the sample size was relatively small 471 for the group analyses (n = 10). Although this sample size was sufficient to confirm 472 previous findings on long-range  $\alpha$ -synchronisation and lateralization index (Sauseng 473 et al., 2005; Thut et al., 2006), the negative results of the group analyses should be 474 interpreted with caution.

#### 475 Fronto-parietal network synchronisation characterises

#### 476 visuospatial attention

477 A result from our study is that long-range  $\alpha$ -synchronisation within the FPN was 478 associated with the consequences of visuospatial attention orienting, in line with its 479 putative role in this cognitive process (Jensen et al. 2015; Sacchet et al. 2015; 480 Doesburg et al. 2009; Siegel et al. 2008). We observed significant increase in 481 contralateral vs. ipsilateral upper  $\alpha$  coherence for targets appearing at the attended 482 location. According to the current attention theories, the mechanism underlying this 483 finding may be inherently related to top-down processing. More specifically, frontal 484 regions such as the frontal eye fields (FEF) and the intraparietal sulcus (IPS) may 485 modulate attention by causing a state of  $\alpha$ -band desynchronisation in the visual cortex 486 contralateral to attended hemifield (Corbetta and Shulman 2002; Kastner and 487 Ungerleider 2000; Helfrich et al. 2018; Capotosto et al. 2009; Marshall et al. 2015). 488 This explanation further aligns with the well-established evidence that contralateral  $\alpha$ -489 power suppression (also reproduced in our results) enables visual stimuli processing 490 in the attended location (Doesburg et al. 2009; Thut et al. 2006; Yamagishi et al. 2003; 491 Babiloni et al. 2006; Foxe and Snyder 2011; Klimesch et al. 2007; Lange et al. 2013), 492 and that cyclic phase-dependent inhibition in low-level visual cortex dictates 493 behavioural performance (i.e., reaction times) (Haegens et al. 2011; Klimesch 2012; 494 Jensen et al. 2014; Samaha et al. 2015; VanRullen 2016). Both accounts fit with the 495 idea that local  $\alpha$ -power and long-range  $\alpha$ -synchronisation may have separate roles in 496 attention and perception (Bonnefond et al. 2017; Palva and Palva 2007, 2011; 497 Sadaghiani and Kleinschmidt 2016).

498 Our results of the increased contralateral synchronisation within the FPN replicate the 499 work of Sauseng et al. (2005) and validate our methodology and analysis pipeline 500 (e.g., time-frequency analysis, synchronisation metric), setting the ground for the 501 intended proof of concept test regarding transference to BCI. However, lateralised 502 fronto-parietal connectivity patterns in attentional and perceptual disposition remain 503 challenged in the literature together with the role of  $\alpha$  power/phase (Ruzzoli, Torralba 504 et al. 2019; van Diepen et al. 2019; Antonov et al. 2020; Keitel et al., 2022). Lobier et 505 al. (2018) found that  $\alpha$ -synchronisation was associated with visuospatial attention but 506 revealed distinct lateralisation patterns regarding the visual system and top-down 507 attentional networks. They showed stronger ipsilateral synchronisation within the 508 visual system (in line with Siegel et al. 2008; Doesburg et al. 2009) but no consistent

509 lateralisation in long-range networks, suggesting their different involvement in 510 visuospatial attention. A study by D'Andrea et al. (2019) found a modulation of 511 frontoparietal  $\alpha$ - $\beta$  cross-frequency synchronisation during attention orienting, but not 512 in  $\alpha$ -synchronisation alone. Further, this cross-frequency connectivity pattern was 513 strongly associated with right hemisphere frontal dominance, in line with Heilman and 514 van den Abell (1980) and Zago et al. (2017). This finding agrees with previous 515 evidence of the crucial role of the right FEF in top-down attentional modulation 516 (Esterman et al. 2015; Hung et al. 2011; Silvanto et al. 2006; Veniero et al., 2021), 517 supported by evidence using TMS (e.g., Capotosto et al. 2009). In light of this evidence 518 and our results, the exact relationship between contralateral frontoparietal  $\alpha$ -519 synchronisation and shifts in attention orienting is still unclear. Positive findings, 520 however, such as the ones in the present study using a target-locked analysis, 521 represent a basis for exploring earlier time windows capable of shedding light on the 522 mechanism underlying FPN  $\alpha$ -synchronisation.

523 Correlations between long-range  $\alpha$ -synchronisation and individual reaction times in 524 visuospatial tasks suggest this neural correlate may be observable at a single-subject 525 level (Lobier et al., 2018). However, significant group-level target-locked dynamics of 526 increased synchrony did not transfer to all individuals in our study. The observed 527 variability may be partially explained by individual anatomical differences in the neural 528 substrate of attention (e.g., superior longitudinal fasciculus) (Marshall et al., 2015). 529 Findings employing magnetic resonance imaging (MRI) suggest that volumetric 530 differences in these structures impact local visual cortex oscillations, leading to 531 variability in EEG traces (Marshall et al. 2015; D'Andrea et al. 2019). However, this 532 variability of individual results is challenging to set in the perspective of previous 533 research simply because published studies do not report single-subject statistics.

534 Ultimately, the outcomes of this study leave an incomplete understanding of whether 535 there is a reliable group effect that does not extend to all individuals or, contrarily, 536 whether individual effects of specific participants are large enough to induce a group-537 level finding in previous research.

#### 538 Lateralized patterns of α-synchronisation appear in target-

#### 539 locked but not cue-locked analysis

540 In our study, long-range  $\alpha$ -synchronisation presented contralateral increases at the 541 post-target (200 to 400 ms, with t = 0 as target appearance) and the pre-target window 542 (-200 to 0 ms), but only the former time window resulted significantly. This result is 543 slightly different from Sauseng et al. (2005), who observed significant increases in 544 contralateral synchronisation within the FPN network at both time windows. However, 545 the numerical differences were in the same direction in both studies, leaving the 546 possibility that statistical significance be just due to a lack of statistical power. Another 547 potential explanation for the absence of significant findings at the pre-target window 548 may be the difference in experimental paradigms. The task employed here had a 549 longer post-cue interval ranging from 2000 to 2500 ms (jittered between trials), 550 compared to Sauseng et al. (2005) (i.e., 600-800 ms). If participants shifted attention 551 at varying times from cue onset up to target appearance, this might explain why we could not capture the effect in anticipatory visuospatial attention. 552

In cueing paradigms, bottom-up integration of cue information through sensory
pathways precedes top-down modulation of visuospatial attention (Simpson et al.,
2011). The temporal course of voluntary directed attention is thought to begin only
after 150 ms from cue onset and involves frontal regions approximately after 350 ms.

557 Furthermore, from 400-500 ms onwards, frontal and parietal regions are thought to be 558 involved in attentional shifting and target discrimination (Simpson et al. 2011). Thus, if 559 the FPN does present direction-specific synchronisation, we anticipated this would 560 appear from about 500 ms after cue onset onwards. Contrary to what we expected, 561 we did not observe any significant contra- to ipsilateral differences in the cue-to-target 562 time windows (500 to 1500 ms after cue onset). Previous studies employing a similar 563 time window showed lateralisation patterns in parietal regions in  $\alpha$  and  $\beta$  bands (Siegel 564 et al. 2008; Pantazis et al. 2009) and frontoparietal lateralisation in low and high-565 frequency bands (Green and McDonald 2008; Gregoriou et al. 2009). Therefore, we 566 extended our cue-locked analysis to other frequencies but again obtained no 567 significant contra- to ipsilateral differences. Note that PLV values were averaged 568 across 200 ms windows, and this excludes, to a certain extent, the confound of frontal 569 and parietal regions having different activation over time. Altogether, despite the 570 evidence across multiple frequencies of synchronisation in the cue-to-target time 571 window, we did not find patterns of lateralised cue-locked connectivity within or outside 572 the  $\alpha$ -band.

573 Our negative results in the cue-locked analysis may align with the notion that late 574 periods after cue onset are associated with direction-specific activity in parieto-575 occipital regions but not in frontal regions (e.g., FEF) (Doesburg et al. 2009; Simpson 576 et al. 2011). Long-range  $\alpha$ -synchronisation may, therefore, be associated to an initial 577 shift of attention (shortly after cue presentation) and later (close to target presentation) 578 to attention maintenance at the directed hemifield (Lobier et al. 2018; Kastner and 579 Ungerleider 2000; Hopfinger et al. 2000; Grent-'t-Jong and Woldorff 2007). This idea 580 resonates with the essential question formerly posed by Sauseng et al. (2005), 581 debating whether frontal involvement in long-range  $\alpha$ -synchronisation is a causative

582 or consequential correlate of posterior activation. Furthermore, it motivated the 583 exploration of cue-locked intervals where bottom-up and top-down processing may 584 have elicited stronger effects on  $\alpha$ -band synchronisation.

585 Finally, to ensure participants correctly lateralised their attention during the cue-to-586 target interval, we carried out a reality check by calculating the  $\alpha$ -power imbalance 587 using the lateralisation index during this period (Thut et al. 2006). There was a clear 588 difference in the averaged lateralisation index during the time course between 500 and 589 1500 ms at group-level. We further employed the lateralisation index to perform an 590 exploratory analysis of its relationship with the difference in  $\alpha$ -synchronisation between 591 contra- and ipsilateral networks. Considering lateralised local  $\alpha$  activity and lateralised 592 long-range  $\alpha$ -synchronisation are both relevant in successful attention orienting, we 593 explored whether these two mechanisms would have had a significant positive 594 correlation. Therefore, individuals with high lateralisation index values should also 595 present lateralised synchronisation within the FPN. In contrast to our expectations, 596 there was no significant correlation between these two metrics, neither at the pre-597 target nor the post-target time windows.

598 Ultimately, we did not observe a significant increase in contralateral long-range  $\alpha$ -599 synchronisation in the five 200 ms bins following cue onset. This time frame offered 600 potential as it occurs much before target appearance and could be robustly employed 601 in a covert visuospatial BCI decoder. By expanding our analysis to several frequencies 602 and carrying out the aforementioned reality checks, we conclude that PLV measured 603 from EEG may not serve as a reliable metric in capturing direction-specific 604 synchronisation from frontal to posterior regions, despite this evidence being present 605 in parietal to occipital synchrony (Doesburg et al. 2009).

#### EEG estimates of long-range $\alpha$ -synchronisation may not

#### 607 serve as a reliable control signal for BCI

608 The use of long-range  $\alpha$ -synchronisation to decode attentional direction yielded 609 chance-level results. We employed 200 ms time bins of contralateral and ipsilateral 610 FPN connectivity as input in an SVM classifier. Non-linear SVMs are widely employed 611 in decoding cognitive neural correlates of behavioural states (Lotte et al., 2007). 612 Furthermore, SVMs outperform other classifiers, such as artificial neural networks, 613 non-linear Bayesian estimators, and recurrent reservoir networks (Astrand et al. 614 2014a). We also employed sLDA and RMDM classifiers, as they have low 615 computational cost, require small training sets, and perform well in real-time 616 applications (Lotte et al., 2018), with no success.

617 Prior work using SVMs, mainly centred around primate models and invasive 618 recordings, successfully decoded the attentional spotlight from frontal sites (Gaillard 619 et al. 2020; Tremblay et al. 2015; Esghaei and Daliri 2014). Clearly, these methods 620 (i.e., LFP, intracranial-EEG) have a higher signal-to-noise ratio (SNR) compared to 621 non-invasive imaging. However, the objective of the present study was to offer a BCI 622 proof of concept using  $\alpha$ -synchronisation as a control signal. Therefore, a non-invasive 623 and portable technique must be employed. Other non-invasive modalities such as 624 functional magnetic resonance imaging (fMRI), where the temporal resolution is too 625 low for real-time implementations, or magnetoencephalography (MEG), where the 626 equipment is expensive and requires a magnetically shielded room (as fMRI), have 627 limited potential transfer in out-of-lab applications. Contrarily, EEG is an affordable 628 imaging modality with a straightforward setup which provides high temporal resolution 629 and portability. However, the inconvenience of using EEG is a low spatial resolution

630 and a low SNR. Despite this, decoders have been commonly employed in EEG-BCI 631 design employing parieto-occipital power changes in  $\alpha$ -band activity to predict covert 632 visuospatial attention tasks (Tonin et al. 2013; Treder et al. 2011; van Gerven et al., 633 2009). The integrated approach between frontal and parieto-occipital attentional 634 decoding based on  $\alpha$ -synchronisation, however, has not been attempted. Here, we 635 found that cue-locked synchronisation enclosed in the FPN  $\alpha$ -band is insufficient to 636 determine the attentional location at EEG single trial level. This may be due to an 637 inherent lack of connectivity in the cue-to-target interval, or else more likely, the poor 638 sensitivity of the EEG to register synchronisation patterns.

639 Another potential reason to explain the failed classification of cue-locked FPN 640 connectivity at single-trial level may be the change in PLV calculation from trial-641 average to single-trial. Standard cognitive research employs multiple trials to estimate 642 consistent findings on electrophysiological markers (M/EEG). Instead, BCIs need 643 robust and accurate estimates in a single-trial fashion and thus require a trade-off 644 between spatial (i.e., single-channel decoding is preferred) and temporal resolution. 645 PLV is a measure of consistency across multiple trials and cannot serve as a single-646 trial control signal. Therefore, we computed PLV across time points within the same 647 trial. This new measure is also referred to in the literature as the inter-site phase 648 clustering (ISPC) and may represent a different underlying process than that captured 649 by classic PLV (Cohen 2015). This prompts the question of whether long-range  $\alpha$ -650 synchronisation is incapable of decoding the attended location, or rather the single-651 trial nature of IPSC over time is responsible for this.

652 In sum, long-range  $\alpha$ -synchronisation within the FPN estimated with EEG may not 653 serve as a control signal for BCI. This limitation may be due to incomplete information

654 on neural correlates due to the lack of cross-frequency analysis or the computational
655 techniques surrounding ISPC over time.

## 656 CONCLUSION

657 We found direction-specific contralateral patterns of upper  $\alpha$ -synchronisation (i.e., 658 PLV) within the FPN following target appearance in a covert visuospatial task. This 659 finding, however, did not extend to pre-target or cue-to-target time windows. The 660 modulatory role of  $\alpha$ -synchronisation in anticipatory attention through frontal, parietal 661 and occipital regions suggests that PLV may not constitute a reliable metric for this 662 top-down visual processing. Furthermore, chance-level classification resulting from 663 using this metric in an SVM indicates that long-range  $\alpha$ -synchronisation computed with 664 EEG may not be a suitable control signal for BCI.

## 665 **REFERENCES**

Antonov, Plamen A.; Chakravarthi, Ramakrishna; Andersen, Søren K. (2020): Too
little, too late, and in the wrong place: Alpha band activity does not reflect an active
mechanism of selective attention. In *NeuroImage* 219, p. 117006. DOI:
10.1016/j.neuroimage.2020.117006.
Asplund, Christopher L.; Todd, J. Jay; Snyder, Andy P.; Marois, René (2010): A
central role for the lateral prefrontal cortex in goal-directed and stimulus-driven
attention. In *Nature neuroscience* 13 (4), pp. 507–512. DOI: 10.1038/nn.2509.

Astrand, Elaine; Enel, Pierre; Ibos, Guilhem; Dominey, Peter Ford; Baraduc, Pierre;
Ben Hamed, Suliann (2014a): Comparison of classifiers for decoding sensory and
cognitive information from prefrontal neuronal populations. In *PloS one* 9 (1),
e86314. DOI: 10.1371/journal.pone.0086314.

Astrand, Elaine; Wardak, Claire; Ben Hamed, Suliann (2014b): Selective visual
attention to drive cognitive brain-machine interfaces: from concepts to
neurofeedback and rehabilitation applications. In *Frontiers in systems neuroscience*8, p. 144. DOI: 10.3389/fnsys.2014.00144.

Babiloni, Claudio; Vecchio, Fabrizio; Bultrini, Alessandro; Luca Romani, Gian;
Rossini, Paolo Maria (2006): Pre- and poststimulus alpha rhythms are related to
conscious visual perception: a high-resolution EEG study. In *Cerebral cortex (New York, N.Y. : 1991)* 16 (12), pp. 1690–1700. DOI: 10.1093/cercor/bhj104.

Baselice, F., Sorriso, A., Rucco, R., & Sorrentino, P. (2018). Phase linearity
measurement: A novel index for brain functional connectivity. IEEE transactions on
medical imaging, 38(4), 873-882.

Benjamini, Yoav; Hochberg, Yosef (1995): Controlling the False Discovery Rate: A
Practical and Powerful Approach to Multiple Testing. In *Journal of the Royal Statistical Society: Series B (Methodological)* 57 (1), pp. 289–300. DOI:
10.1111/j.2517-6161.1995.tb02031.x.

Blankertz, Benjamin; Acqualagna, Laura; Dähne, Sven; Haufe, Stefan; SchultzeKraft, Matthias; Sturm, Irene et al. (2016): The Berlin Brain-Computer Interface:
Progress Beyond Communication and Control. In *Frontiers in neuroscience* 10,
p. 530. DOI: 10.3389/fnins.2016.00530.

Bonnefond, Mathilde; Kastner, Sabine; Jensen, Ole (2017): Communication between
Brain Areas Based on Nested Oscillations. In *eNeuro* 4 (2). DOI:

698 10.1523/ENEURO.0153-16.2017.

699 Capotosto, Paolo; Babiloni, Claudio; Romani, Gian Luca; Corbetta, Maurizio (2009):

700 Frontoparietal cortex controls spatial attention through modulation of anticipatory

alpha rhythms. In *J. Neurosci.* 29 (18), pp. 5863–5872. DOI: 10.1523/jneurosci.053909.2009.

- 703 Clayton, Michael S.; Yeung, Nick; Cohen Kadosh, Roi (2018): The many characters
- 704 of visual alpha oscillations. In *The European journal of neuroscience* 48 (7),
- 705 pp. 2498–2508. DOI: 10.1111/ejn.13747.
- 706 Cohen, Michael X. (2015): Effects of time lag and frequency matching on phase-
- 507 based connectivity. In Journal of neuroscience methods 250, pp. 137–146. DOI:
- 708 10.1016/j.jneumeth.2014.09.005.
- Cohen, Mike X. (2014): Analysing neural time series data: Theory and practice.
  Cambridge, Massachusetts, USA: The MIT Press.
- 711 Corbetta, Maurizio; Shulman, Gordon L. (2002): Control of goal-directed and
- 712 stimulus-driven attention in the brain. In Nature reviews. Neuroscience 3 (3),
- 713 pp. 201–215. DOI: 10.1038/nrn755.
- 714 D'Andrea, Antea; Chella, Federico; Marshall, Tom R.; Pizzella, Vittorio; Romani,
- 715 Gian Luca; Jensen, Ole; Marzetti, Laura (2019): Alpha and alpha-beta phase
- 716 synchronisation mediate the recruitment of the visuospatial attention network through
- 717 the Superior Longitudinal Fasciculus. In *NeuroImage* 188, pp. 722–732. DOI:
- 718 10.1016/j.neuroimage.2018.12.056.
- Doesburg, Sam M.; Bedo, Nicolas; Ward, Lawrence M. (2016): Top-down alpha
  oscillatory network interactions during visuospatial attention orienting. In *NeuroImage*132, pp. 512–519. DOI: 10.1016/j.neuroimage.2016.02.076.
- 722 Doesburg, Sam M.; Green, Jessica J.; McDonald, John J.; Ward, Lawrence M.
- 723 (2009): From local inhibition to long-range integration: a functional dissociation of
- alpha-band synchronisation across cortical scales in visuospatial attention. In *Brain research* 1303, pp. 97–110. DOI: 10.1016/j.brainres.2009.09.069.
- 726 Esghaei, Moein; Daliri, Mohammad Reza (2014): Decoding of visual attention from
- LFP signals of macaque MT. In *PloS one* 9 (6), e100381. DOI:
- 728 10.1371/journal.pone.0100381.
- 729 Esterman, Michael; Liu, Guanyu; Okabe, Hidefusa; Reagan, Andrew; Thai, Michelle;
- 730 DeGutis, Joe (2015): Frontal eye field involvement in sustaining visual attention:
- evidence from transcranial magnetic stimulation. In *NeuroImage* 111, pp. 542–548.
- 732 DOI: 10.1016/j.neuroimage.2015.01.044.
- Foster, Joshua J.; Awh, Edward (2019): The role of alpha oscillations in spatial
  attention: limited evidence for a suppression account. In *Current opinion in psychology* 29, pp. 34–40. DOI: 10.1016/j.copsyc.2018.11.001.
- 736 Foster, Joshua J.; Sutterer, David W.; Serences, John T.; Vogel, Edward K.; Awh,
- Edward (2017): Alpha-Band Oscillations Enable Spatially and Temporally Resolved
- Tracking of Covert Spatial Attention. In *Psychological science* 28 (7), pp. 929–941.
  DOI: 10.1177/0956797617699167.

- Foxe, John J.; Snyder, Adam C. (2011): The Role of Alpha-Band Brain Oscillations
  as a Sensory Suppression Mechanism during Selective Attention. In *Frontiers in*
- 742 *psychology* 2, p. 154. DOI: 10.3389/fpsyg.2011.00154.
- 743 Fries, Pascal (2005): A mechanism for cognitive dynamics: neuronal communication
- through neuronal coherence. In *Trends in cognitive sciences* 9 (10), pp. 474–480.
- 745 DOI: 10.1016/j.tics.2005.08.011.
- Fries, Pascal (2015): Rhythms for Cognition: Communication through Coherence. In *Neuron* 88 (1), pp. 220–235. DOI: 10.1016/j.neuron.2015.09.034.
- Gaillard, Corentin; Ben Hadj Hassen, Sameh; Di Bello, Fabio; Bihan-Poudec, Yann;
  VanRullen, Rufin; Ben Hamed, Suliann (2020): Prefrontal attentional saccades
  explore space rhythmically. In *Nature communications* 11 (1), p. 925. DOI:
  10.1038/s41467-020-14649-7.
- Green, Jessica J.; McDonald, John J. (2008): Electrical Neuroimaging Reveals
  Timing of Attentional Control Activity in Human Brain. In *PLoS Biol* 6 (4), e81. DOI:
  10.1371/journal.pbio.0060081.
- Gregoriou, Georgia G.; Gotts, Stephen J.; Zhou, Huihui; Desimone, Robert (2009):
  High-frequency, long-range coupling between prefrontal and visual cortex during
  attention. In *Science (New York, N.Y.)* 324 (5931), pp. 1207–1210. DOI:
  10.1126/science.1171402.
- Grent-'t-Jong, Tineke; Woldorff, Marty G. (2007): Timing and sequence of brain
  activity in top-down control of visual-spatial attention. In *PLoS Biol* 5 (1), e12. DOI:
  10.1371/journal.pbio.0050012.
- Grossmann, A.; Morlet, J. (1984): Decomposition of Hardy Functions into Square
  Integrable Wavelets of Constant Shape. In *SIAM J. Math. Anal.* 15 (4), pp. 723–736.
  DOI: 10.1137/0515056.
- Haegens, Saskia; Nácher, Verónica; Luna, Rogelio; Romo, Ranulfo; Jensen, Ole
  (2011): α-Oscillations in the monkey sensorimotor network influence discrimination
  performance by rhythmical inhibition of neuronal spiking. In *Proceedings of the National Academy of Sciences of the United States of America* 108 (48), pp. 19377–
  19382. DOI: 10.1073/pnas.1117190108.
- Heilman, K. M.; van den Abell, T. (1980): Right hemisphere dominance for attention:
  the mechanism underlying hemispheric asymmetries of inattention (neglect). In
- 772 *Neurology* 30 (3), pp. 327–330. DOI: 10.1212/wnl.30.3.327.
- Helfrich, Randolph F.; Fiebelkorn, Ian C.; Szczepanski, Sara M.; Lin, Jack J.; Parvizi,
  Josef; Knight, Robert T.; Kastner, Sabine (2018): Neural Mechanisms of Sustained
- 775 Attention Are Rhythmic. In *Neuron* 99 (4), 854-865.e5. DOI:
- 776 10.1016/j.neuron.2018.07.032.

Hjorth, B. (1975). An on-line transformation of EEG scalp potentials into orthogonal
source derivations. Electroencephalography and clinical neurophysiology, 39(5),
526-530.

- Hopfinger, J. B.; Buonocore, M. H.; Mangun, G. R. (2000): The neural mechanisms
  of top-down attentional control. In *Nature neuroscience* 3 (3), pp. 284–291. DOI:
  10.1038/72999.
- Hung, June; Driver, Jon; Walsh, Vincent (2011): Visual selection and the human
  frontal eye fields: effects of frontal transcranial magnetic stimulation on partial report
  analysed by Bundesen's theory of visual attention. In *J. Neurosci.* 31 (44),
- 786 pp. 15904–15913. DOI: 10.1523/jneurosci.2626-11.2011.
- 787 Jensen, Ole; Bonnefond, Mathilde; Marshall, Tom R.; Tiesinga, Paul (2015):
- Oscillatory mechanisms of feedforward and feedback visual processing. In *Trends in neurosciences* 38 (4), pp. 192–194. DOI: 10.1016/j.tins.2015.02.006.
- Jensen, Ole; Gips, Bart; Bergmann, Til Ole; Bonnefond, Mathilde (2014): Temporal
  coding organised by coupled alpha and gamma oscillations prioritise visual
- processing. In *Trends in neurosciences* 37 (7), pp. 357–369. DOI:
- 793 10.1016/j.tins.2014.04.001.
- Kastner, S.; Ungerleider, L. G. (2000): Mechanisms of visual attention in the human
  cortex. In *Annual review of neuroscience* 23, pp. 315–341. DOI:
- 796 10.1146/annurev.neuro.23.1.315.
- Keitel, C., Ruzzoli, M., Dugué, L., Busch, N. A., & Benwell, C. S. (2022). Rhythms in
  cognition: The evidence revisited. European Journal of Neuroscience, 55(11-12),
  2991-3009.
- Klimesch, Wolfgang (1999): EEG alpha and theta oscillations reflect cognitive and
  memory performance: a review and analysis. In *Brain Research Reviews* 29 (2-3),
  pp. 169–195. DOI: 10.1016/s0165-0173(98)00056-3.
- Klimesch, Wolfgang (2012): α-band oscillations, attention, and controlled access to
  stored information. In *Trends in cognitive sciences* 16 (12), pp. 606–617. DOI:
  10.1016/j.tics.2012.10.007.
- Klimesch, Wolfgang; Sauseng, Paul; Hanslmayr, Simon (2007): EEG alpha
  oscillations: the inhibition-timing hypothesis. In *Brain Research Reviews* 53 (1),
  pp. 63–88. DOI: 10.1016/j.brainresrev.2006.06.003.
- Lachaux, Jean-Philippe; Rodriguez, Eugenio; Martinerie, Jacques; Varela, Francisco J. (1999): Measuring phase synchrony in brain signals. In *Hum. Brain Mapp.* 8 (4),
- 811 pp. 194–208. DOI: 10.1002/(sici)1097-0193(1999)8:4%3C194::aid-
- 812 hbm4%3E3.0.co;2-c.
- Lange, Joachim; Oostenveld, Robert; Fries, Pascal (2013): Reduced occipital alpha power indexes enhanced excitability rather than improved visual perception. In *J.*
- 815 *Neurosci.* 33 (7), pp. 3212–3220. DOI: 10.1523/jneurosci.3755-12.2013.

- Lobier, Muriel; Palva, J. Matias; Palva, Satu (2018): High-alpha band
- 817 synchronisation across frontal, parietal and visual cortex mediates behavioral and
- 818 neuronal effects of visuospatial attention. In *NeuroImage* 165, pp. 222–237. DOI:
- 819 10.1016/j.neuroimage.2017.10.044.
- Lotte, F., Congedo, M., Lécuyer, A., Lamarche, F., & Arnaldi, B. (2007). A review of
  classification algorithms for EEG-based brain–computer interfaces. Journal of neural
  engineering, 4(2), R1.
- Lotte, F., Bougrain, L., Cichocki, A., Clerc, M., Congedo, M., Rakotomamonjy, A., &
  Yger, F. (2018). A review of classification algorithms for EEG-based brain–computer
  interfaces: a 10 year update. Journal of neural engineering, 15(3), 031005.
- Makeig, Scott; Bell, Anthony J.; Jung, Tzyy-Ping; Sejnowski, Terrence J. (1995):
  Independent Component Analysis of Electroencephalographic Data. In : Proceedings
- 828 of the 8th International Conference on Neural Information Processing Systems.
- 829 Cambridge, MA, USA: MIT Press (NIPS'95), pp. 145–151.
- Maris, Eric; Oostenveld, Robert (2007): Nonparametric statistical testing of EEG- and
  MEG-data. In *Journal of neuroscience methods* 164 (1), pp. 177–190. DOI:
  10.1016/j.jneumeth.2007.03.024.
- Marshall, Tom R.; O'Shea, Jacinta; Jensen, Ole; Bergmann, Til O. (2015): Frontal
  eye fields control attentional modulation of alpha and gamma oscillations in
  contralateral occipitoparietal cortex. In *J. Neurosci.* 35 (4), pp. 1638–1647. DOI:
  10.1523/jneurosci.3116-14.2015.
- Meyer, Marlene; Lamers, Didi; Kayhan, Ezgi; Hunnius, Sabine; Oostenveld, Robert
  (2021): Enhancing reproducibility in developmental EEG research: BIDS, clusterbased permutation tests, and effect sizes. In *Developmental cognitive neuroscience*52, p. 101036. DOI: 10.1016/j.dcn.2021.101036.
- Mostame, Parham; Moharramipour, Ali; Hossein-Zadeh, Gholam-Ali; BabajaniFeremi, Abbas (2019): Statistical Significance Assessment of Phase Synchrony in
  the Presence of Background Couplings: An ECoG Study. In *Brain topography* 32 (5),
  pp. 882–896. DOI: 10.1007/s10548-019-00718-8.
- Padfield, Natasha; Zabalza, Jaime; Zhao, Huimin; Masero, Valentin; Ren, Jinchang
  (2019): EEG-Based Brain-Computer Interfaces Using Motor-Imagery: Techniques
- and Challenges. In Sensors (Basel, Switzerland) 19 (6). DOI: 10.3390/s19061423.
- 848 Palva, Satu; Palva, J. Matias (2007): New vistas for alpha-frequency band
- 849 oscillations. In *Trends in neurosciences* 30 (4), pp. 150–158. DOI:
- 850 10.1016/j.tins.2007.02.001.
- 851 Palva, Satu; Palva, J. Matias (2011): Functional roles of alpha-band phase
- 852 synchronisation in local and large-scale cortical networks. In *Frontiers in psychology*
- 853 2, p. 204. DOI: 10.3389/fpsyg.2011.00204.

- eNeuro Accepted Manuscript
- 854 Pantazis, Dimitrios; Simpson, Gregory V.; Weber, Darren L.; Dale, Corby L.; Nichols,
- 855 Thomas E.; Leahy, Richard M. (2009): A novel ANCOVA design for analysis of MEG
- data with application to a visual attention study. In *NeuroImage* 44 (1), pp. 164–174.
  DOI: 10.1016/j.neuroimage.2008.07.012.
- 858 Pashler, H. (1999): The Psychology of Attention: MIT Press (A Bradford book).
- 859 Available online at https://books.google.es/books?id=w\\_4MyczgUEcC.
- 860 Petersen, Steven E.; Posner, Michael I. (2012): The attention system of the human 861 brain: 20 years after. In *Annual review of neuroscience* 35, pp. 73–89. DOI:
- 862 10.1146/annurev-neuro-062111-150525.
- Posner, M. I. (1980): Orienting of attention. In *The Quarterly journal of experimental psychology* 32 (1), pp. 3–25. DOI: 10.1080/00335558008248231.
- Rihs, Tonia A.; Michel, Christoph M.; Thut, Gregor (2007): Mechanisms of selective
  inhibition in visual spatial attention are indexed by alpha-band EEG synchronisation.
  In *The European journal of neuroscience* 25 (2), pp. 603–610. DOI: 10.1111/j.14609568.2007.05278.x.
- Ruzzoli, Manuela; Torralba, Mireia; Morís Fernández, Luis; Soto-Faraco, Salvador
  (2019): The relevance of alpha phase in human perception. In *Cortex; a journal devoted to the study of the nervous system and behavior* 120, pp. 249–268. DOI:
  10.1016/j.cortex.2019.05.012.
- Sacchet, Matthew D.; LaPlante, Roan A.; Wan, Qian; Pritchett, Dominique L.; Lee,
  Adrian K. C.; Hämäläinen, Matti et al. (2015): Attention drives synchronisation of
  alpha and beta rhythms between right inferior frontal and primary sensory neocortex.
  In *J. Neurosci.* 35 (5), pp. 2074–2082. DOI: 10.1523/jneurosci.1292-14.2015.
- Sadaghiani, Sepideh; Kleinschmidt, Andreas (2016): Brain Networks and αOscillations: Structural and Functional Foundations of Cognitive Control. In *Trends in cognitive sciences* 20 (11), pp. 805–817. DOI: 10.1016/j.tics.2016.09.004.
- Samaha, Jason; Bauer, Phoebe; Cimaroli, Sawyer; Postle, Bradley R. (2015): Topdown control of the phase of alpha-band oscillations as a mechanism for temporal
  prediction. In *Proceedings of the National Academy of Sciences of the United States*of *America* 112 (27), pp. 8439–8444. DOI: 10.1073/pnas.1503686112.
- Sauseng, P.; Klimesch, W.; Stadler, W.; Schabus, M.; Doppelmayr, M.; Hanslmayr,
  S. et al. (2005): A shift of visual spatial attention is selectively associated with human
  EEG alpha activity. In *The European journal of neuroscience* 22 (11), pp. 2917–
  2926. DOI: 10.1111/j.1460-9568.2005.04482.x.
- Siegel, Markus; Donner, Tobias H.; Oostenveld, Robert; Fries, Pascal; Engel,
  Andreas K. (2008): Neuronal synchronisation along the dorsal visual pathway
  reflects the focus of spatial attention. In *Neuron* 60 (4), pp. 709–719. DOI:
- 891 10.1016/j.neuron.2008.09.010.

- eNeuro Accepted Manuscript
- Silvanto, Juha; Lavie, Nilli; Walsh, Vincent (2006): Stimulation of the human frontal
  eye fields modulates sensitivity of extrastriate visual cortex. In *Journal of neurophysiology* 96 (2), pp. 941–945. DOI: 10.1152/jn.00015.2006.
- Simpson, Gregory V.; Weber, Darren L.; Dale, Corby L.; Pantazis, Dimitrios;
  Bressler, Steven L.; Leahy, Richard M.; Luks, Tracy L. (2011): Dynamic activation of
  frontal, parietal, and sensory regions underlying anticipatory visual spatial attention.
- 898 In *J. Neurosci.* 31 (39), pp. 13880–13889. DOI: 10.1523/jneurosci.1519-10.2011.
- Thatcher, R. W., Soler, E. P., North, D. M., & Otte, G. (2020). Independent
  Components Analysis "Artifact Correction" Distorts EEG Phase in Artifact Free
  Segments. J Neurol Neurobiol, 6(4), 5-7.
- Thut, Gregor; Nietzel, Annika; Brandt, Stephan A.; Pascual-Leone, Alvaro (2006):
  Alpha-band electroencephalographic activity over occipital cortex indexes
  visuospatial attention bias and predicts visual target detection. In *The Journal of neuroscience : the official journal of the Society for Neuroscience* 26 (37), pp. 9494–
  906 9502. DOI: 10.1523/JNEUROSCI.0875-06.2006.
- Tonin, L.; Leeb, R.; Del R Millán, J. (2012): Time-dependent approach for single trial
  classification of covert visuospatial attention. In *Journal of neural engineering* 9 (4),
  p. 45011. DOI: 10.1088/1741-2560/9/4/045011.
- 910 Tonin, L.; Leeb, R.; Sobolewski, A.; Del Millán, J. R. (2013): An online EEG BCI
- 911 based on covert visuospatial attention in absence of exogenous stimulation. In
- 912 Journal of neural engineering 10 (5), p. 56007. DOI: 10.1088/1741-
- 913 2560/10/5/056007.
- Treder, Matthias S.; Bahramisharif, Ali; Schmidt, Nico M.; van Gerven, Marcel A. J.;
  Blankertz, Benjamin (2011): Brain-computer interfacing using modulations of alpha
  activity induced by covert shifts of attention. In *Journal of neuroengineering and rehabilitation* 8, p. 24. DOI: 10.1186/1743-0003-8-24.
- 918 Tremblay, Sébastien; Doucet, Guillaume; Pieper, Florian; Sachs, Adam; Martinez-
- 919 Trujillo, Julio (2015): Single-Trial Decoding of Visual Attention from Local Field
- 920 Potentials in the Primate Lateral Prefrontal Cortex Is Frequency-Dependent. In J.
- 921 *Neurosci.* 35 (24), pp. 9038–9049. DOI: 10.1523/jneurosci.1041-15.2015.
- van Diepen, Rosanne M.; Foxe, John J.; Mazaheri, Ali (2019): The functional role of
  alpha-band activity in attentional processing: the current zeitgeist and future outlook.
  In *Current opinion in psychology* 29, pp. 229–238. DOI:
  10.1016/j.copsyc.2019.03.015.
- van Gerven, Marcel; Jensen, Ole (2009): Attention modulations of posterior alpha as
  a control signal for two-dimensional brain-computer interfaces. In *Journal of neuroscience methods* 179 (1), pp. 78–84. DOI: 10.1016/j.jneumeth.2009.01.016.
- 929 VanRullen, Rufin (2016): Perceptual Cycles. In *Trends in cognitive sciences* 20 (10),
  930 pp. 723–735. DOI: 10.1016/j.tics.2016.07.006.

- 931 Veniero, D., Gross, J., Morand, S., Duecker, F., Sack, A. T., & Thut, G. (2021). Top932 down control of visual cortex by the frontal eye fields through oscillatory realignment.
  933 Nature communications, 12(1), 1-13.
- Vigué-Guix, I., Moris Fernandez, L., Torralba Cuello, M., Ruzzoli, M., & Soto-Faraco,
  S. (2022). Can the occipital alpha-phase speed up visual detection through a real-
- 936 time EEG-based brain-computer interface (BCI)?. European Journal of
- 937 Neuroscience, 55(11-12), 3224-3240.
- 938 Yamagishi, Noriko; Callan, Daniel E.; Goda, Naokazu; Anderson, Stephen J.;
- 939 Yoshida, Yoshikazu; Kawato, Mitsuo (2003): Attentional modulation of oscillatory
- 940 activity in human visual cortex. In NeuroImage 20 (1), pp. 98–113. DOI:
- 941 10.1016/s1053-8119(03)00341-0.
- 942 Zago, Laure; Petit, Laurent; Jobard, Gael; Hay, Julien; Mazoyer, Bernard; Tzourio-
- 943 Mazoyer, Nathalie et al. (2017): Pseudoneglect in line bisection judgement is
- 944 associated with a modulation of right hemispheric spatial attention dominance in
- 945 right-handers. In Neuropsychologia 94, pp. 75–83. DOI:
- 946 10.1016/j.neuropsychologia.2016.11.024.
- 947

## 948 **LEGENDS**

949 Figure 1. Experimental design and response rates. (A) Schematic trial 950 representation. A black fixation cross in the middle of the screen and two squares 951 (to-be-attended locations) at the bottom left, and bottom right positions were displayed 952 continuously. At the beginning of each trial, participants were instructed to gaze at the 953 fixation cross. After 200 ms (fixation period), an auditory cue appeared for 100 ms (cue 954 period) indicating which hemifields participants must attend (75% validity). After a 955 jittered interstimulus interval of 2000  $\pm$  500 ms, a target appeared at the targeted 956 location during 50 ms (target period). Participants had to report first if they had seen 957 the target (detection task), and after 1000 ms, the location of the target (left/right 958 discrimination task) during 1500 ms. An intertrial interval (ITI) of 1000 ms followed, 959 and a new trial began (Adapted from Torralba et al. 2016). (B) Response rates for 960 detected and discriminated trials (HITS) related to attended and unattended 961 trials. Black lines over violin plots represent the mean value. Both overall performance 962 (top) and right/left hemifields (bottom) are shown. White dots indicate individual values 963 (adapted from Torralba et al. 2016).

964 Figure 2. Target-locked results. (A) Target-locked results of the phase-coupling 965 for attended left (light blue) and attended right (dark blue) in FM-PL and FM-PR 966 **networks.** The lower panels depict the cross-trial average time course (± shaded 967 SEM) of PLV in both conditions (attended left and attended right). Upper panels 968 present the binned violin plots (mean and median) of the pre-target window (-200 to 0 969 ms) and the post-target window (200 to 400 ms); p < 0.05. (B) Target-locked results 970 collapsed as either ipsilateral (FM-PL network and attended left; FM-PR and 971 attended right) or contralateral (FM-PR network and attended left; FM-PL and 972 **attended right).** The lower panel shows the cross-trial average time course (± shaded 973 SEM) of PLV in ipsilateral (light grey) and contralateral (dark grey) conditions. The 974 upper panel exhibits the distribution of individual PLV with a violin plot, superimposed 975 by the mean and the contra- to ipsilateral differences between individual PLV; \**p* < 976 0.05. Individual results with PLV are found in Figure 2-1, and thoes with PLM are found 977 in Figure 2-2.

978 Figure 3. Cue-locked results. (A) Group-level results of upper-alpha PLV. Upper 979 panel shows phase coupling for ipsilateral (light grey) and contralateral (dark grey) 980 sides in time-windows of 200 ms from the cue-locked interval (500 ms to 1500 ms after 981 cue presentation). Lower panel shows mean and standard error of the mean (SEM) of 982 the PLV values. Individual results are shown in Figure 3-1. (B) Exploratory analysis 983 of PLV differences. Group-level temporal evolution of the z-scored difference 984 between contralateral and ipsilateral PLV for each frequency band (2.4 - 42 Hz with 985 16 logarithmic steps). Z-score values range from -0.03 to 0.03. Individual results are 986 shown in Figure 3-2.

987 Figure 4. Classification outcomes. (A) Cross-time PLV reality check. Replication 988 of results from Fig. 2 calculating PLV across time points rather than across trials. 989 Individual results are shown in Figure 4-1. (B) Optimisation results of gamma and 990 margin parameters of the Gaussian kernel SVM. Ten-fold validation accuracies with 991 varying margin values (x-axis) and gamma values (y-axis). Inset shows a detailed view of the z-axis. (C) Confusion matrix of the classification outcomes for one 992 993 participant. Y-axis represents ground truth labels (attended right or attended left) and 994 x-axis represents the classifier's outcomes. Percentages represent the fraction of 995 correctly classified trials of each condition (i.e., each row sums to 100%). Under the

39

996 percentage is the gross number of classified trials. Results with additional classifiers997 such as sLDA and RDMD are shown in Figure 4-2.

998 Figure 5. Lateralisation index reality check. (A) Averaged lateralization index for 999 attended left (light blue) and attended right (dark blue; \*p < 0.05; \*\*p < 0.01). 1000 White dots denote individual scores, and horizontal line indicates the group mean. (B) 1001 Lateralisation index (mean ± SEM) over time. Solid lines and shaded areas 1002 represent mean and standard error of the mean (SEM) interval, respectively. Dots on 1003 in the x-axis denote the significant difference over time between attended left (light 1004 blue) and attended right (dark blue) via cluster-based permutation test. Individual 1005 results are shown in Figure 5-1. (C-D) Lateralisation indexes and the difference of 1006 contra- to ipsilateral PLV for attended left (light blue) and attended right (dark 1007 blue) at the pre-target window (C) and the post-target window (D). At the pre-1008 target the correlations for attended right (r = -0.33, p > 0.05) and attended left (r = -0.33, p > 0.05) and attended left (r = -0.33, p > 0.05) and attended left (r = -0.33, p > 0.05) and attended left (r = -0.33, p > 0.05) and attended left (r = -0.33, p > 0.05) and attended left (r = -0.33, p > 0.05) and attended left (r = -0.33, p > 0.05) and attended left (r = -0.33, p > 0.05) and attended left (r = -0.33, p > 0.05) and attended left (r = -0.33, p > 0.05) and attended left (r = -0.33, p > 0.05) and attended left (r = -0.33, p > 0.05) and attended left (r = -0.33, p > 0.05) and attended left (r = -0.33, p > 0.05) and attended left (r = -0.33, p > 0.05) and attended left (r = -0.33, p > 0.05) and attended left (r = -0.33, p > 0.05) and r = -0.33. 1009 0.19. p > 0.05) did not reach significance and neither did the correlations for attended 1010 right (r = -0.38, p > 0.05) and attended left r = -0.46, p > 0.05) at the post-target window. 1011 Crosses denote participants with a significant effect in PLV contra-ipsi differences at 1012 the pre-target window (-200 to 0 ms; P05) and the post-target window (200 to 400 ms; 1013 P02 and P07). Dots represent the rest of the participants.

eNeuro Accepted Manuscript

## 1014 EXTENDED FIGURE LEGENDS

Figure 2-1. Individual results of target-locked PLV index. Violin plots represent the phase locking values (PLV) averaged over the pre-target (-200 to 0 ms, t = 0 as target appearance) and post-target time window (200 to 400 ms). Ipsilateral (FM-PL network and *attended left*; FM-PR and *attended right*) or contralateral (FM-PR network and *attended left*; FM-PL and *attended right*) scenarios are exhibited as either light grey or dark grey, respectively. \**p* < 0.05, \*\**p* < 0.01, \*\*\**p* < 0.001.

**Figure 2-2. Individual results of target-locked PLM index.** Violin plots represent the phase linearity measurement (PLM) over the pre-target (-200 to 0 ms, t = 0 as target appearance) and post-target time window (200 to 400 ms). Ipsilateral (FM-PL network and *attended left*; FM-PR and *attended right*) or contralateral (FM-PR network and *attended left*; FM-PL and *attended right*) scenarios are exhibited as either light grey or dark grey, respectively. \**p* < 0.05, \*\**p* < 0.01, \*\*\**p* < 0.001.

Figure 3-1. Individual results of upper-alpha cue-locked PLV analysis. Violin plots represent the phase locking values (PLV) averaged over the five time windows (500 to 700, 700 to 900, 1100 to 1300, and 1300 to 1500 ms; t = 0 as cue appearance). lpsilateral or contralateral scenarios are exhibited as either light grey or dark grey, respectively. \*p < 0.05, \*\*p < 0.01.

Figure 3-2. Individual results of cue-locked exploratory PLV analysis. Differences
of contra- to ipsilateral PLV are represented over frequencies (2.4 – 42 Hz in 16
logarithmic steps) as a percentage of change regarding the cross-frequency mean of
each individual.

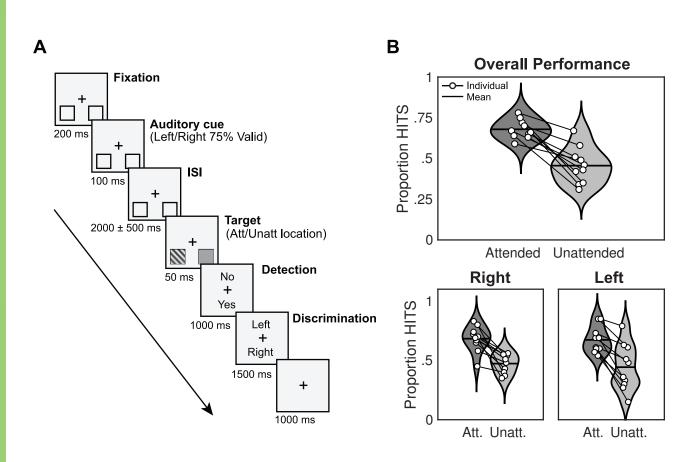
Figure 4-1. Individual results of target-locked cross-time PLV. Violin plots
represent the phase locking values (PLV) obtained by calculating PLV as consistency
throughout the pre-target (-200 to 0 ms) and post-target (200 to 400 ms) time windows.
Ipsilateral or contralateral scenarios are exhibited as either light grey or dark grey,
respectively.

1041 Fig 4-2. Additional classifier analysis. (A) Shrinkage linear discriminant analysis.

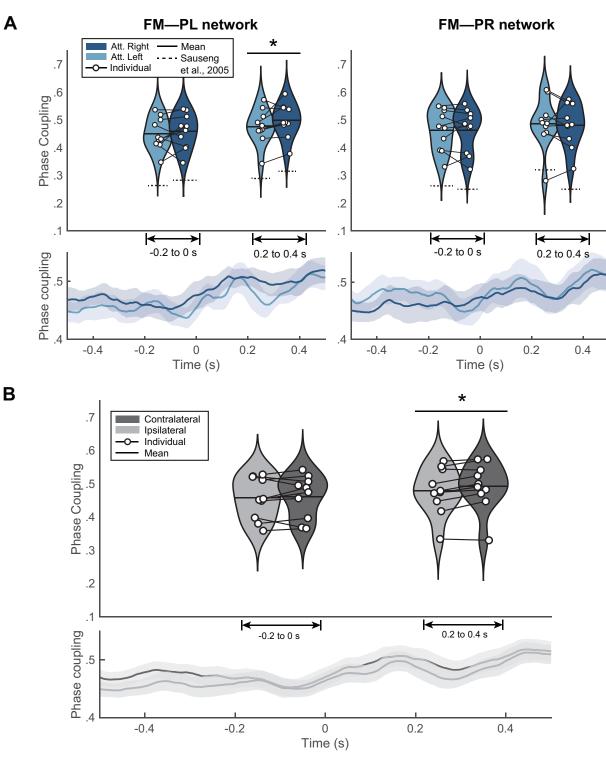
1042 The leftmost panel reveals how classification error is not modulated by gamma1043 parameter of number of predictors. The rightmost panel presents the confusion matrix.

1044 **(B)** Riemannian minimum distance to the mean classification results.

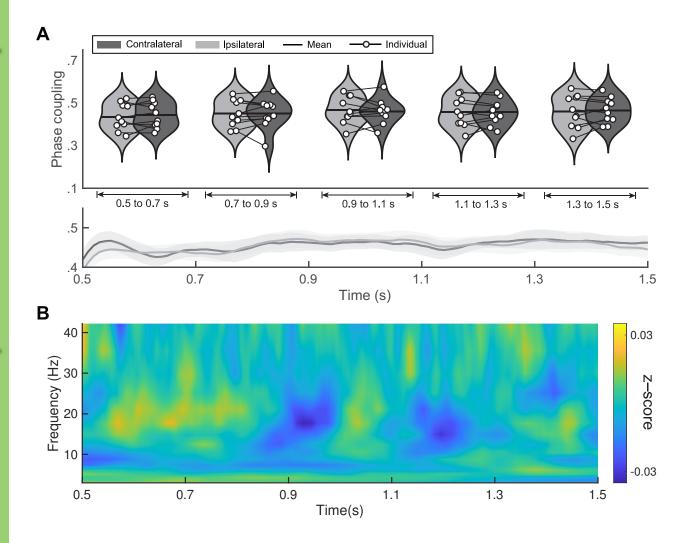
Figure 5-1. Individual results of lateralisation index. Violin plots represent the averaged lateralised index for *attended left* (light blue) and *attended right* trials (dark blue) over the cue-locked time window. Shaded plots represent lateralisation over time (mean  $\pm$  SEM). Dots on in the x-axis denote the significant differences over time between *attended left* and *attended right* via cluster-based permutation test. \**p* < 0.05, \*\**p* < 0.01, \*\*\**p* < 0.001.







l



## eNeuro Accepted Manuscript

